

## Nuclear $E1$ Overtones

J. H. CARVER, D. C. PEASLEE, AND R. B. TAYLOR  
*Australian National University, Canberra, Australia*

(Received May 18, 1961; revised manuscript received April 19, 1962)

The magnitude and energy distribution of nuclear  $E1$  cross sections are considered in the light of recent evidence for a large, positive collective shift in the giant resonance energy. Two secondary mechanisms appear relevant: quasi-deuteron or two-particle effects; and overtones of the fundamental  $E1$  resonance, representing vibration of the nucleus as a whole. These overtones must exist on any mechanical model, and one object of the present paper is to point out their probable importance for real nuclei. Four types of rough experimental data now available indicate a first overtone intensity of order 25% relative to the fundamental. The parameters obtained are applied to yield (a) an estimate of  $W_0 \sim 60$  MeV for the energy at which quasi-deuteron effects become predominant; (b) predicted curves of  $\int \sigma dW$  to finite upper limits, suitable for immediate comparison with experiment, in contrast to sum rules that require infinite upper limits in principle; (c) a corrected estimate  $\gamma \sim 1$  for the nuclear exchange force parameter, indicating two-body forces in the nucleus that are relatively weak (attractive) in odd states; and (d) an improved formula for nuclear polarizability.

### I. INTRODUCTION AND SUMMARY

EVIDENCE has been presented<sup>1</sup> that the collective energy shift proposed<sup>2,3</sup> for nuclear  $E1$  absorption is in fact quite large and sensibly independent of mass number,  $\Delta \approx 7.5$  MeV, in contrast with the free-particle contribution to the giant resonance energy,  $\hbar\omega \approx 40A^{-1/3}$  MeV. The purpose of the present article is to explore what this result implies for the magnitude and energy distribution of the  $E1$  cross section, particularly in the region just above the giant resonance. Two mechanisms have previously been suggested as relevant: absorption by quasi-deuterons,<sup>4</sup> reflecting strong two-particle correlations in the nuclear ground state; and overtones of the giant resonance,<sup>5,6</sup> representing oscillations by the nucleus as a whole. In practice, however, both mechanisms have so far seemed of doubtful significance for the bulk of photonuclear data, which is at energies  $E_\gamma \lesssim 30$  MeV. Two-particle correlations are the most obvious explanation for failure of giant resonance cross sections to attain the sum rule limits. But earlier calculations indicated that the quasi-deuteron and giant resonance integrated cross sections should have the same  $A$  dependence, in contrast to experiment, where the discrepancy between giant resonance and sum rules is particularly large ( $\sim 50\%$ ) for light nuclei and practically vanishes for heavy nuclei. On previous estimates the nuclear  $E1$  overtones had energies well above 30 MeV, even for the heaviest nuclei, so that they were of little practical interest. Moreover, preliminary computations suggested very small cross sections for

the overtones, of order a few percent that in the giant resonance.

Introduction of the constant shift  $\Delta$  seems to change this situation and make both mechanisms of immediate concern for data already available at  $E_\gamma \lesssim 30$  MeV, as well as for prospective measurements in the  $E_\gamma = 30$ –60 MeV range. The argument is elaborated in the following sections but in outline is quite simple. The sum rule limit corresponding to a peak energy of  $W_1 = (40A^{-1/3} + \Delta)$  MeV is  $\int \sigma dW \sim (40A + \Delta A^{4/3})$  for an ideal harmonic oscillator (i.h.o.) without two-particle correlations. The appearance in this formula of a substantial term varying as  $A^{4/3}$  means that the removal of some cross sections to higher energies by quasi-deuteron effects—for which  $\int \sigma_{qd} dW \sim A$ —will become relatively less important for large  $A$ ; or that the fraction of the sum rule limit contained in the giant resonance integral will systematically increase with  $A$ , as observed. With regard to the overtones, the presence of  $\Delta$  implies that the first  $E1$  overtone should occur not at  $W_3 \approx 3W_1$ , but nearer to  $W_3 \approx 3(W_1 - \Delta_1)$ . For light nuclei this energy is still considerably above 30 MeV but for heavy nuclei it is definitely not; thus if the first overtone at  $W_3$  contains any appreciable cross section, it also will help to make  $\int_0^{30 \text{ MeV}} \sigma dW$  approach the sum rule limit much better for heavy than for light nuclei.

Any model that yields a giant resonance must necessarily imply an infinite series of overtones. It should be of interest in principle to look for these overtones as confirming further details of the model; conversely, one would generally expect the overtones to be useful for interpreting experiment. In spite of this, the question of nuclear  $E1$  overtones has received very little serious consideration in the literature—much less than quasi-deuteron effects, for example. It is therefore appropriate to begin by devoting Sec. II to a discussion of overtones. Since the discussion is exploratory in character, it will be sufficient to use a simplified model: non-matching harmonic oscillators. This makes preservation of the sum rule limit quite explicit while at the

<sup>1</sup> J. H. Carver and D. C. Peaslee, *Phys. Rev.* **120**, 2155 (1960). Equations from this reference are prefixed with the numeral I.

<sup>2</sup> R. A. Ferrell, *Bull. Am. Phys. Soc.* **1**, 135 (1956).

<sup>3</sup> G. E. Brown and M. Bolsterli, *Phys. Rev. Letters* **3**, 462 (1959).

<sup>4</sup> J. S. Levinger, *Phys. Rev.* **84**, 43 (1951); *Nuclear Photo-disintegration* (Oxford University Press, New York, 1960).

<sup>5</sup> M. Danos and H. Steinwedel, *Z. Naturforsch.* **6a**, 217 (1951).

<sup>6</sup> D. H. Wilkinson, *Physica* **22**, 1039 (1956). This reference does not explicitly mention overtones, but it includes in Table II a matrix element calculated for the transition  $1l$  to  $2(l+1)$ , which is a principal component of the first overtone.

same time allowing the cross section not to concentrate entirely in the fundamental resonance. The magnitude of the absorption in overtones is left an arbitrary parameter to be fitted from experiment.

Section III determines a fit to the magnitude of the overtones from a survey of available data, including some data presented here for the first time (Appendix A). It appears reasonable to ascribe to the first overtone a harmonic integral averaging about 25% of that in the giant resonance. Although this is a relatively large intensity, experimental resolution of the first overtone has not been achieved so far. Whether this is due to a very great intrinsic width for the overtone or—as seems more likely—to instrumental difficulties, there can be no doubt that a contribution of this magnitude is significant for understanding integrated cross sections.

In Sec. IV the results of the present analysis are applied. The quasi-deuteron and overtone corrections make possible the first predicted curve of  $\int_0^{30 \text{ MeV}} \sigma dW$  as a function of  $A$ . Even an approximate formula relating to actual experiment may have advantages over a sum rule that requires guessing a “measured value” of  $\sigma$  from  $E_\gamma \approx 30 \text{ MeV}$  to  $E_\gamma \rightarrow \infty$ ! The same corrections permit a revised estimate of the exchange parameter  $\gamma$  for two-body forces<sup>1</sup> associated with  $\Delta$ ; the new value is in better accord with other estimates and indicates an effective two-body potential that is strongly attractive in even states, weakly attractive in odd states. One can also obtain a rough estimate for the energy at which quasi-deuteron effects begin to predominate for E1 absorption in nuclear matter,  $W_0 \approx 60 \text{ MeV}$ , and an improved formula for nucleon polarizability.

## II. OVERTONE FORMULAS

Although E1 overtones were first noticed for the classical, vibrating-fluid model,<sup>5,7</sup> we shall discuss them entirely in terms of the shell model. Here, E1 excitation may in principle promote a nucleon to the next, 3rd next, 5th next, . . . shell in accord with parity conservation; such transitions will be called “1-, 3-, 5-, . . . quantum jumps.” For the i.h.o. the associated frequencies are in the ratio  $\omega_1:\omega_3:\omega_5:\dots=1:3:5:\dots$ , while the corresponding matrix elements are in the ratio  $1:0:0:\dots$ . Of course the i.h.o. is unrealistic with respect to these features and must be modified.

Consider first the frequencies: Here the principal modification is the addition of a collective shift  $\Delta$  to the i.h.o. energy. Thus, for a 1-quantum jump the energy is (I26)

$$W_1 = \hbar\omega_1 + \Delta_1 \approx (40A^{-1/3} + 7.5) \text{ MeV}. \quad (1)$$

The constant shift  $\Delta_1 \approx 7.5 \text{ MeV}$  arises from two-nucleon exchange forces and can be expressed (I16) as an integral over the momenta of initial and final nuclear

states. For a 3-quantum jump the mean momentum difference between states is about three times that for a 1-quantum jump; a smooth dependence of the effective exchange potential on momentum transfer would suggest a reduction of  $\Delta_3$  by a factor of 2 or 3 relative to  $\Delta_1$ . The coefficient of  $A^{-1/3}$  in Eq. (1) also contains a slight factor of enlargement<sup>1</sup> that can be expected to diminish for higher levels of excitation. In the 3-quantum jump it may therefore be more appropriate to take  $\omega_3 = 3\omega_1$ , where  $\hbar\omega_1 \approx 38A^{-1/3}$  is the shell model spacing (I29). Then one has

$$W_3 \approx (115A^{-1/3} + 3) \text{ MeV}, \quad (2)$$

and, correspondingly,

$$W_5 \approx 190A^{-1/3} \text{ MeV}, \quad (3)$$

where the shift term  $\Delta_5$  is assumed negligible in comparison.

The most conspicuous lack of realism in the i.h.o. is its radial selection rule that concentrates the entire E1 absorption in 1-quantum jumps. This can be corrected by using i.h.o. functions with different range parameters  $a$  and  $b$  for initial and final states; physically, the assumption  $b > a$  should to some extent reflect the unbound condition of the final state. Then one has

$$\begin{aligned} (R_N^1/R_N)^2 &= \left( \frac{2ab}{a^2+b^2} \right)^{2N+5} = \eta^{N+5/2}, \\ (R_N^3/R_N)^2 &= (N+5/2)(1-\eta)\eta^{N+5/2}, \\ (R_N^5/R_N)^2 &= \frac{1}{2}(N+5/2)(N+7/2)(1-\eta)^2\eta^{N+5/2}, \end{aligned} \quad (4)$$

where  $R_N$  is the radial matrix element of  $r$  for the transition ( $l=N$ )  $\rightarrow$  ( $l+1, N+1$ ) of the i.h.o. when  $b=a$  and  $l, N$  are the orbital and principal quantum numbers. The radial matrix elements when  $b \neq a$  are  $R_N^1, R_N^3, R_N^5, \dots$ , for transitions ( $l=N$ )  $\rightarrow$  ( $l+1, N+1$ ), ( $l+1, N+3$ ), ( $l+1, N+5$ ), . . . . Although only the maximum  $l$  values are considered, these make by far the dominant contribution in any shell, so that Eq. (4) may be taken to indicate the corresponding ratios of harmonic integrals,  $H_n = \int \sigma_n dW/W$  for the  $n$ -quantum jump. These are normalized to the total harmonic integral  $H_0$ , which is identical with the 1-quantum jump for the i.h.o. Then defining  $\xi = (N+5/2)(1-\eta)$ , one has

$$\begin{aligned} H_3/H_1 &= \xi, \\ H_5/H_1 &= \frac{1}{2}\xi^2[1 + (N+5/2)^{-1}], \\ H_1/H_0 &= [1 - \xi(N+5/2)^{-1}]^{N+5/2}. \end{aligned} \quad (5)$$

From Eq. (5) one may infer that in the limit of large  $N$  and small  $\xi$ ,

$$H_{2n+1}/H_0 \rightarrow \xi^n e^{-\xi}/n!. \quad (6)$$

This provides a set of  $H_{2n+1}$  expressible in terms of a

<sup>1</sup> Lord Rayleigh, *Theory of Sound* (MacMillan and Company, Ltd., London, 1878), Chap. 17.

single parameter  $\xi$  and preserving the sum rule,

$$\sum_{n=0}^{\infty} H_{2n+1} = H_0. \quad (7)$$

The asymptotic relation (6) will suffice for present considerations.

Since overtones are characteristic of the nucleus as a whole, the formulas above are essentially independent of two-particle correlations in the ground state, which can accordingly be taken into account simply by correcting  $H_0$ . In the formula (I31, I12)

$$H_0 \sim \langle D^2 \rangle_{00} = \frac{1}{4} \sum_j \langle (z^j)^2 \rangle_{00} + \frac{1}{4} \sum_{i \neq j} \langle \tau_z^i \tau_z^j z^i z^j \rangle_{00}, \quad (8)$$

only the second term is affected by two-particle correlations, and the important ones for the  $E1$  photoeffect are between neutron and proton with  $\tau_z^i \tau_z^j = -1$ . The correlation region of  $z^i z^j$  will be fixed by the short range of nuclear forces and will be largely independent of  $A$ ; but the  $\sum_{i \neq j}$  will introduce the usual factor  $NZ/A \sim A$  for the number of  $n$ - $p$  pairs. The harmonic integral without correlations, denoted by  $H_{00}$ , varies as  $A^{4/3}$ ; thus, the effect of correlation is to yield

$$H_0 = H_{00}(1 - CA^{-1/3}), \quad (9)$$

where  $C$  is a positive constant to be determined empirically. The correction term in Eq. (9) is of course associated with quasi-deuteron contributions to the photo-nuclear cross section,<sup>4</sup> which reduce  $H_0 = \int \sigma dW/W$  by shifting some of the cross section to higher energies. This process tends to mitigate the sharpness of the giant resonance and overtones by spreading smoothly over a wide energy range some of the absorption cross section that would otherwise have resided in the peaks.

The corrections for  $E1$  overtones and quasi-deuteron effects are here expressed in terms of two unspecified

constants,  $\xi$  and  $C$ ; comparison with experiment in the next section indicates that neither constant is negligibly small.<sup>8</sup>

### III. COMPARISON WITH EXPERIMENT

#### (a) Photoproton Reactions

Photoproton reactions on heavy elements appear to offer a favorable opportunity for observing 3-quantum jumps with present equipment. Photoneutron measurements with bremsstrahlung sources would be plagued by resolution difficulties with respect to the fundamental giant resonance; but for photoprotons the high Coulomb barrier in heavy elements ( $\sim 10$  MeV) should effectively suppress both direct and compound nucleus proton emission from the  $W_1$  peak while having much less effect at  $W_3$ . Photoproton cross sections for heavy elements are, in fact, observed to be very small in the region of the giant resonance and to reach maxima in the high energy tails.

In order to obtain more accurate information about such cross sections, experiments were performed as described in Appendix A. The  $(\gamma, p)$  reactions on  $W^{189}$ ,  $W^{186}$ , and  $Hg^{201}$  were studied by means of induced radioactivity up to  $\gamma$ -ray energies of 32 MeV. The  $(\gamma, n)$  cross section on  $W^{186}$  was also measured for comparison. Table I summarizes the results.

It is of interest to compare the  $W^{186}(\gamma, p)$  and  $(\gamma, n)$  cross sections in the high-energy region ( $E_\gamma \gtrsim 23$  MeV) where the Coulomb barrier is no longer the dominant effect for photoproton emission. Because of the long half-life of the pure negatron emitter produced in the  $W^{186}(\gamma, n)W^{185}$  (74 day) reaction we were unable to measure the detailed shape of the cross section for this reaction. We assume that the shape of the  $W^{186}(\gamma, n)W^{185m}$  (1.8 min) cross section, with its large high-energy tail, faithfully represents the shape of the total  $(\gamma, n)$  cross section and normalize this cross section with the measured yield ratio of 76-day  $W^{185}$  to 1.8-min  $W^{185m}$  at 32 MeV. Since the 1.8-min  $W^{185m}$  yield is only  $\sim 1\%$  of the total  $(\gamma, n)$  yield, this procedure is not free from objection. It may be noted, however, that similar large tails have been observed in other  $(\gamma, n)$  cross sections.<sup>9,10</sup> The relative  $W^{186}(\gamma, p)$  and  $W^{186}(\gamma, n)$  cross sections

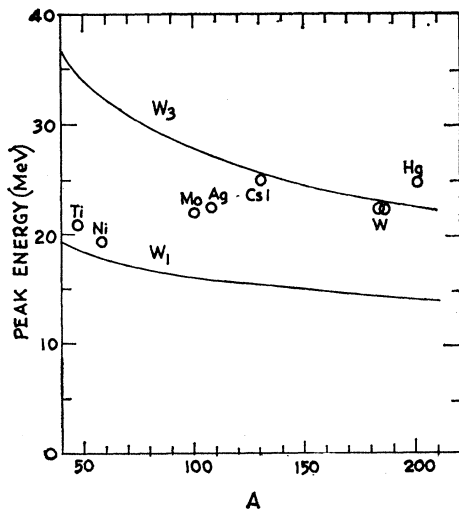


FIG. 1. Photoproton peak energies for medium and heavy nuclei.

<sup>8</sup> The quite small value of  $\xi \approx 3\%$  obtained for the square well model (see reference 6) resulted from a very specific choice of boundary conditions for the initial and final radial functions: namely, both vanishing at the nuclear radius. This leads to a specially simplified formula for the radial overlap integrals,  $D^{\pm} = 4xy(x^2 - y^2)^2$ , where  $x$  and  $y$  are the appropriate roots of  $j(z) = 0$  for the initial and final states. A procedure more in keeping with our ignorance on such matters is to allow an arbitrary phase  $\delta$  in the final wave function and then to average  $\xi$  over a range of  $\delta$ . We have made sample calculations of this type with square well wave functions and have found  $\sigma_3/\sigma_1$  ratios an order of magnitude larger than in reference 6. See R. B. Taylor, thesis, Australian National University, 1961 (unpublished).

<sup>9</sup> J. H. Carver, R. D. Edge and K. H. Lokan, Proc. Phys. Soc. (London) **A70**, 415 (1957); J. H. Carver and W. Turchinetz, *ibid.* **71**, 613 (1958).

<sup>10</sup> J. H. Carver and W. Turchinetz, Proc. Phys. Soc. (London) **73**, 110 (1959).

TABLE I. Photonuclear cross sections from Appendix A.

Reaction	Integrated cross section <sup>a</sup> $\int_0^{30} dE$ (MeV-mb)	Peak energy <sup>b</sup> (MeV)
$W^{186}(\gamma, p)Ta^{185}$ (50 min)	55	22.5
$W^{186}(\gamma, n)W^{185}$ (74 day)	3500	14
$W^{186}(\gamma, n)W^{185}$ (1.8 min)	40	14
$W^{184}(\gamma, p)Ta^{183}$ (5.2 day)	65	22.5
$Hg^{201}(\gamma, p)Au^{200}$ (48 min)	40	25

<sup>a</sup> Mean errors of  $\pm 20\%$  for all values.

<sup>b</sup> Mean errors of  $\pm 1$  MeV for all values.

integrated for the high-energy region are

$$\int_{23}^{31} \sigma(\gamma, p) dW / \int_{23}^{31} \sigma(\gamma, n) dW = 0.05 \pm 0.02. \quad (10)$$

Figure 1 indicates the peak position of the  $(\gamma, p)$  cross section as a function of mass number  $A$ , including present results and those of other measurements.<sup>10-12</sup> The positions assigned to the 1-quantum and 3-quantum resonances are also plotted; it is seen that with increasing Coulomb barrier the  $(\gamma, p)$  peak moves gradually from  $W_1$  to  $W_3$ . Peak energies substantially intermediate on this plot, as for Mo and Ag, are still mainly indicative of 3-quantum jumps, since the  $W_1$  peak is presumably narrower than  $W_3$ . Thus, the  $(\gamma, p)$  peak position can tend toward  $W_1$  even though most of the cross section is still contributed by  $W_3$ . In this situation the  $(\gamma, p)$  cross section should be quite asymmetric, with a mean energy higher than the peak energy. We accordingly regard  $A \sim 90-100$  as a transition region: For lighter nuclei, the  $(\gamma, p)$  reaction proceeds mainly through  $W_1$ ; for heavier nuclei, mainly through  $W_3$ .

Figure 2 shows the ratio

$$r = \left[ \int \sigma_p dW / W \right] / \left[ \int \sigma_1 dW / W \right] \approx p(H_3/H_1) = p\xi, \quad (11)$$

including present and other<sup>12-14</sup> results for nuclei where  $(\gamma, p)$  is supposed to be a 3-quantum effect. Here  $p$  is the fraction of  $W_3$  absorption that results in proton emission. An estimate of  $p$  suitable for present purposes is the following: Proton emission by the compound nucleus is assumed to be negligible, so that  $p$  is the probability of direct proton escape relative to compound nucleus formation. The rate of compound nucleus formation is  $2W/\hbar$ , where  $W$  is the absorptive part of the optical model potential for the escaping proton; the rate of proton escape is  $v/d$ , where  $v$  is the mean proton

<sup>11</sup> R. Sherwood and W. Turchinets (to be published); K. H. Lokan, Proc. Phys. Soc. (London) **73**, 697 (1959).

<sup>12</sup> F. Ferrero, A. O. Hanson, P. Malvano, and C. Tribuno, Nuovo cimento **6**, 585 (1957).

<sup>13</sup> R. B. Taylor, Nuclear Phys. **19**, 453 (1960).

<sup>14</sup> W. C. Barber and V. J. Vanhuysse, Nuclear Phys. **16**, 361 (1960).

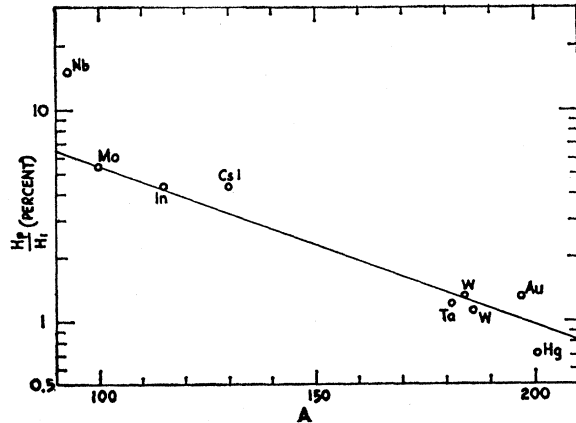


FIG. 2. Harmonic integrated  $(\gamma, p)$  cross sections for heavy nuclei expressed as a percentage of the total harmonic cross section integrated over the first peak:  $r = H_3/H_1 = [\int \sigma_p dW / W] / [\int \sigma_1 dW / W]$ .

velocity and  $d$  is the average distance the proton has to move in order to escape. Since E1 excitation concerns mainly protons in the outer shell,  $d \approx 2F$  ( $1F = 10^{-13}$  cm), and we take  $v \approx 0.3c$ . Then  $p = \hbar v P / 2dW$ , where  $P$  is the Coulomb barrier penetrability, computed for a rather large nuclear radius with  $r_0 = 1.5 F$ . Taking  $W \approx 9$  MeV and a width of 8 MeV for the  $W_3$  peak, we obtain  $p \approx 3\%$  for Pb,  $p \approx 15\%$  for Sn. For intermediate nuclei we interpolate a linear variation of  $\log p$  with  $A$ , which gives a value of  $p = 4.5\%$  for  $A = 186$ , in accord with the measurement in Eq. (10). The solid line in Fig. 2 is drawn on this basis and corresponds to the constant value

$$\xi = 0.3. \quad (12)$$

### (b) Direct Resolution of Measured Cross Sections

Further information on the quantity  $\xi$  can be obtained by attempting to resolve favorable cases of measured  $\gamma$ -absorption cross sections into two peaks centered at  $W_1$  and  $W_3$  and computing the integrals  $H_1$  and  $H_3$  directly. The values (accuracy of order 30%) found in this way<sup>9-13</sup> are

$$\begin{aligned} \xi &= 0.2 \text{ for Ta}^{181} \\ &= 0.3 \text{ for Pr}^{141} \\ &= 0.25 \text{ for Ni}^{58}. \end{aligned} \quad (13)$$

### (c) Fast Neutrons

Measurements of fast neutron emission<sup>12,15</sup> indicate, with some uncertainty, that this process accounts for about 10% of the total yield. If one ascribes these neutrons entirely to direct emission from  $W_3$  and multiplies by a corrective factor  $(1 + 2Wd/\hbar v) \approx 1.5$  to

<sup>15</sup> G. Cortini, C. Milone, A. Rubbino, and F. Ferrero, Nuovo cimento **9**, 85 (1958); S. Cavalloar, V. Emma, C. Milone, and A. Rubbino, *ibid.* **9**, 736 (1958); L. B. Aull, W. O. Whitehead, and G. C. Reinhardt, Nuclear Phys. **13**, 292 (1959).

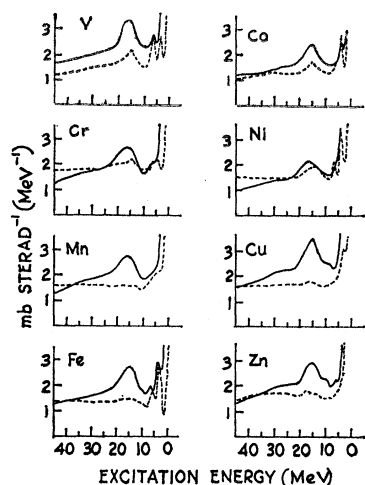


FIG. 3. Inelastic scattering of 185-MeV protons according to Tyrén and Maris.<sup>16</sup> Full line for scattering angle of 10°. Dotted line for scattering angle of 18° (Co, Mn, Fe, Cu, Zn) and 14° (V, Co, Ni).

allow for those neutrons in the 3-quantum peak that did not escape directly but formed a compound nucleus, the 3-quantum yield is of order 15% of the total. Thus,  $\xi e^{-\xi} \approx 0.15$ , or

$$\xi \approx 0.2. \quad (14)$$

#### (d) High-Energy Proton Scattering

Another indication is provided by inelastic scattering of 185 MeV protons<sup>16</sup> at small angles. Here the 1-quantum peak is quite apparent, and an elementary theoretical estimate<sup>17</sup> of Coulomb excitation shows that the integral of this peak, after subtracting background, should be proportional to  $H_1/\theta^2$ , where  $\theta$  is the (small) deviation angle of the protons. In Fig. 3 are reproduced the published curves at 10° (solid) and 18° (dashed) for nuclei in which  $W_3$  should be well above  $W_1$  yet still within range of the experiments. We take the difference between the solid and dashed curves as a simple measure of  $\int \sigma dW/W$ . For five of the eight nuclei (Co, Cu, Zn, Mn, and Fe) it is possible to discern, in addition to the large  $W_1$  peak, something attributable to  $W_3$ ; the values of  $\xi$  estimated by comparing areas between the curves are

$$\xi \approx 0.25 \pm 0.05. \quad (15)$$

This range of values fairly describes all the pieces of information<sup>18</sup> collected above in Eqs. (12)–(14).

<sup>16</sup> H. Tyrén and Th. A. J. Maris, *Nuclear Phys.* **7**, 24 (1958).

<sup>17</sup> M. Kawai and T. Terasawa, *Progr. Theoret. Phys. (Kyoto)* **22**, 513 (1959).

<sup>18</sup> On the classical model of vibrating fluids the first  $E2$  transition occurs between the fundamental and first overtone  $E1$  transitions; its cross section would predominate over the  $E1$  overtones. This raises the question whether the experimental evidence for 3-quantum jumps may not consist mostly of wrongly identified  $E2$  transitions. The nuclear collective model seems to describe  $E2$  transitions quite adequately, however, and for highly deformed nuclei it predicts that the integral  $I_2 = \int \sigma(E2)W^{-3}dW$  will be exhausted except for terms of order  $1/A$  by the transitions (for

#### (e) Direct Observation of $W_3$ in Light Nuclei

A recent measurement<sup>19</sup> of  $C^{12}(\gamma, p)2He^4$  shows distinct peaks around 44 and 64 MeV. Regarded as components of a split 3-quantum peak, these indicate a value of  $W_3 \approx 50$  MeV in accord with Eq. (2). Similar studies of light nuclei ( $A \lesssim 40$ ) should offer the best opportunity for resolving  $W_3$  from  $W_1$ .

### IV. APPLICATION AND DISCUSSION

#### (a) Quasi-Deuteron Parameters

According to the remarks above the harmonic integral in the 1-quantum peak (I35) is expressible as

$$H_1 = \int \sigma_1 dW/W = \frac{1}{2} \pi^2 \alpha a_0^2 e^{-\xi} A^{4/3} (1 - CA^{-1/3}), \quad (16)$$

where  $\alpha = 1/137$  and  $a_0^2 = a^2 A^{-1/3}$  is a fixed range parameter (I11) for i.h.o. nuclear ground states. The novel feature of Eq. (16) is that it relates to an immediately observed quantity  $H_1$  rather than to the total harmonic integral over all energies, which is not completely measurable. An empirical<sup>20</sup> fit of Eq. (16) is shown in Fig. 4, where it appears that

$$C \approx 1 \quad (17)$$

and  $e^{-\xi} a_0^2 \approx \frac{2}{3} F^2$ . In the previous section the empirical value of  $\xi$  appeared to be of order 0.25, so that

$$a_0^2 \approx 0.85 F^2. \quad (18)$$

One can also make a rough estimate of the energy  $W_0$  at which quasi-deuteron effects become important. Let  $\delta H_0 = H_0 - H_{00}$ ; then by Eqs. (16)–(18)

$$\delta H_0 = \frac{1}{2} \pi^2 \alpha a_0^2 (-CA) \approx -0.3A \text{ mb}. \quad (19)$$

even-even nuclei) with  $\Delta K = 0, 2$ , which lie at energies of a few MeV or less. Of course this model is not perfect, and the strong  $W^{-3}$  weighting factor would make the integral  $I_2$  depend very little on high-energy  $E2$  transitions; but one may still expect the  $E2$  admixture in the  $W_3$  region to be small, except perhaps for nuclei near closed shells where the  $E2$  transition energies increase markedly. Experimentally one could look at the angular distribution of photoprotons from the  $W_3$  peak to see the degree of forward-backward asymmetry, which is indicative of  $E1$ – $E2$  interference. There is very little direct evidence on this point, the most relevant measurements probably being  $(\gamma, p)$  angular distributions on heavy elements at 40 MeV.<sup>14</sup> Here there is definite evidence of  $E1$ – $E2$  mixtures in the  $W_3$  region. The distributions also contain substantial isotropic components, so that a complete analysis would be required before the ratio of total cross sections  $\sigma(E2)/\sigma(E1)$  could be determined. The ratio of observed  $\sin^2 \theta$  to  $\sin^2 \theta$  terms suggests, however, that  $\sigma(E2)$  is generally an order of magnitude smaller than  $\sigma(E1)$  in this energy region.

<sup>19</sup> V. V. Balashov and V. N. Fetisov, *Nuclear Phys.* **27**, 337 (1961).

<sup>20</sup> R. Montalbetti, L. Katz, and J. Goldemberg, *Phys. Rev.*, **91**, 659 (1958); P. F. Yergin and B. P. Fabricand, *ibid.* **104**, 1334 (1956); J. H. Carver and K. H. Lokan, *Australian J. Phys.* **10**, 312 (1957); E. G. Fuller, B. Petrie, and M. S. Wiess, *Phys. Rev.* **112**, 554 (1958); J. H. Carver and W. Turchinetz, *Proc. Phys. Soc. (London)* **73**, 585 (1959); E. G. Fuller and Evans Hayward (to be published); N. W. Tanner, G. C. Thomas, and W. E. Mayerhof, *Nuovo cimento* **14**, 257 (1959); S. G. Cohen, P. S. Fisher, and E. K. Warburton, *Phys. Rev. Letters* **3**, 433 (1959) and *Phys. Rev.* **121**, 858 (1961); L. D. Cohen, A. K. Mann, B. J. Patton, K. Reibel, W. E. Stephens, and E. J. Winhold, *ibid.* **104**, 108 (1956).

Another form is to write

$$\delta H_0 \approx \left( \frac{1}{W_d} - \frac{1}{W_h} \right) \int_{W_0}^{\infty} \sigma_{qd} dW = \left( 1 - \frac{W_d}{W_h} \right) \int_{W_0}^{\infty} \frac{\sigma_{qd} dW}{W}, \quad (20)$$

expressing the notion that the quasi-deuteron effect removes some cross section  $\sigma_{qd}$  from the 1-, 3-, 5-, ... quantum peaks (harmonic energy  $W_h$ ) to a higher energy of harmonic mean value  $W_d > W_0$ , characteristic of quasi-deuteron absorption at energies exceeding  $W_0$ . Using the relation<sup>4</sup>  $\sigma_{qd} \approx 2A\sigma_d$ , where  $\sigma_d$  is the free deuteron cross section, one finds agreement between Eqs. (19) and (20) at

$$W_0 \approx 60 \text{ MeV}. \quad (21)$$

Of course quasi-deuteron effects do not really show a sharp threshold, but Eq. (21) should at least show the general region where they start to predominate.

In Eq. (21) we have used the harmonic mean energy given by the present analysis,

$$W_h = \sum_{n=0}^{\infty} W_{2n+1} (H_{2n+1}/H_0) \approx (57A^{-1/3} + 6.5) \text{ MeV}. \quad (22)$$

using the parameters of Eqs. (1)–(3), (15)–(18). This considerably exceeds the value taken in reference 1 and means that  $|W_h - W_1| \lesssim W_1$  rather than  $|W_h - W_1| \ll W_1$ . This change does not entail any alteration in previous qualitative ideas, however, as the exact numerical value of  $W_h$  was nowhere essential to the argument.

### (b) Cross Section Integrals to Finite Energy

A formula like Eq. (16) would be even more useful for the direct integral  $\int \sigma_1 dW$ , for in this case there may be a rather large difference between the infinite integral given by sum rules and the integral measured over any

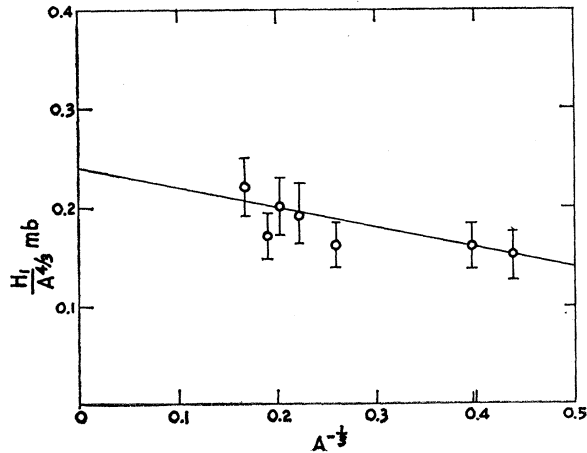


FIG. 4. Harmonic total cross sections,  $H_1 = \int \sigma_1 dW / W$ , for closed shell nuclei integrated over the 1-quantum peak. The full line corresponds to Eqs. (16) and (17) of the text, i.e.,  $H_1 = (0.24A^{4/3} - 0.22A) \text{ mb}$ .

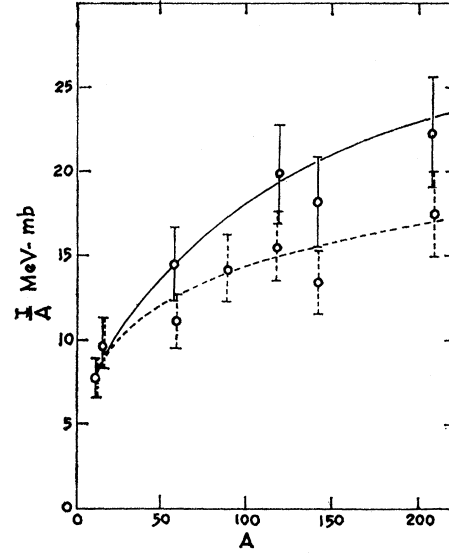


FIG. 5. Total cross section  $I = \int \sigma dW$ , integrated over the first peak (dashed line) and to a fixed upper limit of 30 MeV (solid line). Experimental points for the same nuclei as in Fig. 4.

finite range. It is accordingly of interest to compare with observation the 1-quantum estimate

$$\int \sigma_1 dW \approx W_1 H_1, \quad (23)$$

with  $W_1 H_1$  taken from Eqs. (1), (16), (17). Figure 5 compares the left-hand side of Eq. (23) with the integrated yields over the  $W_1$  peak for a number of nuclei; the agreement appears satisfactory on the average.

Although Eq. (23) gives the integrated cross section to a finite upper limit, this limit is variable. Greater immediacy of experimental comparison would be achieved with a curve calculated to a finite upper limit, say  $\int_0^{30 \text{ MeV}} \sigma dW$ . This is also approximated in Fig. 5 by adding contributions from the fundamental and first overtones only, with  $\Gamma_1 = 5 \text{ MeV}$ ,  $\Gamma_3 = 10 \text{ MeV}$ , Breit-Wigner shapes, and the parameters of Eqs. (1), (2), (15). The agreement with experiment is again satisfactory.

### (c) Correction to Nuclear Exchange Parameter

Most numerical parameters of reference 1 remain essentially unchanged: The formulas (I26) and (I29) for  $W_1$  and the shell model spacing  $E_s$  can be justified empirically; and the range parameter of Eq. (18) turns out to be the same as obtained in (I34).

The principal change from reference 1 is in the estimate of the exchange parameter

$$y = \frac{2(3A_{01} + A_{10} - 3A_{11} - A_{00})}{9A_{11} + 3A_{10} + 3A_{01} + A_{00}}, \quad (24)$$

TABLE II. Summary of reactions investigated.

Abundance of target nucleus	Reaction	Threshold <sup>a</sup> (MeV)	Half-life <sup>b</sup> of product nucleus	Principal <sup>b</sup> decay modes
28.4%	$W^{186}(\gamma, p)Ta^{185}$	8.2	50 min	$\beta^-$ , $\gamma$ 175, 130, 235 keV, x ray
28.4%	$W^{186}(\gamma, n)W^{185}$	7.2	74 day	$\beta^-$ , no $\gamma$
28.4%	$W^{186}(\gamma, n)W^{185m}$		1.8 min	I.T., $\gamma$ 130, 165 keV, x ray
30.6%	$W^{184}(\gamma, p)Ta^{183}$	7.7	5.2 day	$\beta^-$ , many $\gamma$ 's, strongest 246 keV; x ray
13.2%	$Hg^{201}(\gamma, p)Au^{200}$	7.7	48 min	$\beta^-$ , $\gamma$ 1.13, 0.39 MeV

<sup>a</sup> F. Everling, L. A. Konig, J. H. E. Mattauch, and A. H. Wapstra, *Nuclear Phys.* **18**, 529 (1960).

<sup>b</sup> D. Strominger, J. H. Hollander, and G. T. Seaborg, *Revs. Modern Phys.* **30**, 585 (1958); *Nuclear Data Sheets*, National Academy of Sciences, National Research Council (U. S. Government Printing Office, Washington, D. C.).

where  $A_{TS}$  are the parameters of the effective two-nucleon potential in terms of total isotopic and real spin. In place of (I22) we should now write

$$W_1 - \hbar^2/Ma^2 = W_1 - 40A^{-1/3} \approx 7.5 \text{ MeV} = -B'(gV). \quad (25)$$

The numerical constant  $B'$  is to be computed as from (I13–I19), but it no longer has the previous value  $B_0 \approx 0.25$  because of the following modifications: The excited state functions  $\psi_{i+1}$  and  $\psi_{i'+1}$  in (I18) should refer to an i.h.o. with oscillator parameter  $b \neq a$ , the latter holding for  $\psi_i, \psi_{i'}$ . Thus,  $B'$  contains a factor  $e^{-\xi}$ . Probably even more significant, the quasi-deuteron correlations that reduce  $H_1$  must also reduce the constant  $B'$ . It seems very difficult to estimate this

reduction *a priori*, but a crude empirical estimate is the following: For medium to heavy nuclei ( $A^{1/3} \approx 5$ ), the reduction of  $H_1$  is about 20% according to Eq. (17). For these same nuclei ratio of exchange to direct contributions to  $\int \sigma_1 dW$  is of order  $0.2A^{1/3} \approx 1$ . If an over-all reduction of 20% in  $\int \sigma_1 dW$  is assumed to arise entirely from the exchange term, as suggested by the model, the reduction in the exchange term must be of order 40%. Applying these factors,  $B' \approx 0.6e^{-\xi}B_0 \approx 0.1$ ; and (I36) is correspondingly altered to

$$y \sim 1 \text{ (error of order a factor 2)}. \quad (26)$$

This value of  $y$  is larger than in reference 1 and no longer indicates a strongly attractive odd potential effective between two nucleons in nuclear matter.<sup>21</sup>

#### (d) Nuclear Polarizability

The electric polarizability of the nucleus, denoted here by  $\bar{\alpha}$  to avoid confusion with the fine structure constant, is given<sup>4</sup> by

$$\bar{\alpha} = 2e^2 \sum_k \frac{|D_{0n}|^2}{E_n - E_0} = \frac{\hbar c}{2\pi^2} \int \frac{\sigma dW}{W^2}. \quad (27)$$

Historically, this was the first method used to estimate the mean energy of photonuclear absorption<sup>22</sup> by calculating  $\bar{\alpha}$  on a classical, two-fluid model of the nuclear ground state. Since this procedure must omit the effects of exchange forces that give rise to  $\Delta$ , it now seems more appropriate to reverse the argument and employ the formulas above to evaluate the right-hand side of Eq. (27), thus obtaining a nonclassical expression for  $\bar{\alpha}$ . We approximate

$$\begin{aligned} \bar{\alpha} &= \frac{\hbar c}{2\pi^2} \sum_{n=0}^{\infty} H_{2n+1}(W_{2n+1})^{-1} \\ &\approx 7 \times 10^{-3} A^{5/3} (1 - A^{-1/3}) (1 + 0.2A^{1/3})^{-1} F^3, \quad (28) \end{aligned}$$

by Eqs. (1)–(5), (15)–(18). This expression has a more complicated  $A$  dependence than that previously given,

<sup>21</sup> The preliminary forms of the Barker mixture quoted in reference 1 did not quite encompass  $y \sim 1$ ; but the final values, given in F. C. Barker, *Phys. Rev.* **122**, 572 (1961), include a range around  $A_{10}/A_{01} = 0.4$  that is fully compatible with  $y \sim 1$ .

<sup>22</sup> A. Migdal, *J. Phys. (USSR)* **8**, 331 (1944).

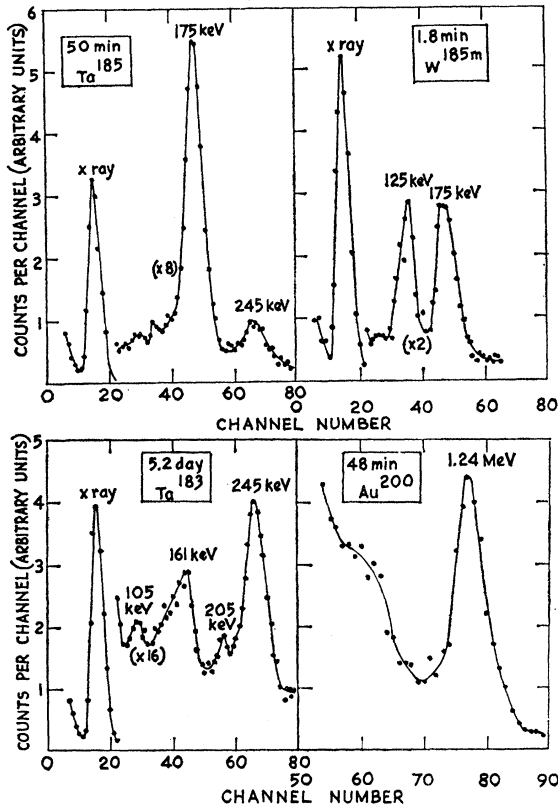


FIG. 6. Observed gamma-ray spectra of  $Ta^{185}$ ,  $W^{185m}$ ,  $Ta^{183}$ , and  $Au^{200}$ .

but for an average value of  $A^{1/3} = 5$  the numerical value is about the same. The condition that  $\bar{\alpha}$  be less than for a perfectly conducting sphere of nuclear radius limits the applicability of Eq. (28) to  $A^{1/3} \lesssim 4 \times 10^2$ , which is, of course, satisfied in practice.

#### APPENDIX A. PHOTODISINTEGRATION MEASUREMENTS ON TUNGSTEN AND MERCURY

This section describes experiments using radioactive detection to study the photodisintegration of tungsten and mercury. The following photoproton cross sections have been measured:  $W^{186}(\gamma, p)Ta^{185}$  (50 min),  $W^{184}(\gamma, p)Ta^{183}$  (5.2 day) and  $Hg^{201}(\gamma, p)Au^{200}$  (48 min). For  $W^{186}$  it is also possible to study the  $(\gamma, n)$  cross section by means of the reactions  $W^{186}(\gamma, n)W^{185}$  (74 day) and  $W^{186}(\gamma, n)W^{185m}$  (1.8 min); in this way, one obtains a direct comparison of the photoproton and photoneutron cross sections for the same target nucleus.

The reactions investigated are listed in Table II together with their threshold energies and some of the properties of the radioactive product nuclei.

Elemental samples of tungsten and mercury of natural isotopic abundance were irradiated with bremsstrahlung produced by the Canberra 33-MeV electron synchrotron for periods of from 2 min to 12 h, depending on the half-lives of the product nuclei. Tantalum foils were irradiated simultaneously in order to monitor the irradiations by means of the 3.15-h  $Ta^{180m}$  activity produced by the  $Ta^{181}(\gamma, n)$  reaction. Absolute yields were obtained by comparing the  $(\gamma, n)$  yields from copper and tantalum foils in a separate series of short irradiations using the results of Berman and Brown<sup>23</sup> for the  $Cu^{63}(\gamma, n)Cu^{62}$  cross section.

A  $1\frac{1}{2}$ -in.-diam  $\times$  1-in.-long Be-window NaI(Tl) spectrometer was used to observe the low-energy gamma-rays of 50-min  $Ta^{185}$ , 1.8-min  $W^{185}$ , and 5.2-day  $Ta^{183}$ . The higher energy gamma rays of 48-min  $Au^{200}$  were observed with a  $1\frac{1}{2}$ -in.-diam  $\times$  2-in.-long NaI(Tl) spectrometer. Typical gamma-ray spectra for these isotopes are shown in Fig. 6. Appropriate corrections were made for the relative efficiency of the spectrometers for these gamma rays and for the annihilation radiation of  $Cu^{62}$  produced in the standard  $Cu^{63}(\gamma, n)$

<sup>23</sup> A. I. Berman and K. L. Brown, Phys. Rev. **96**, 83 (1954).

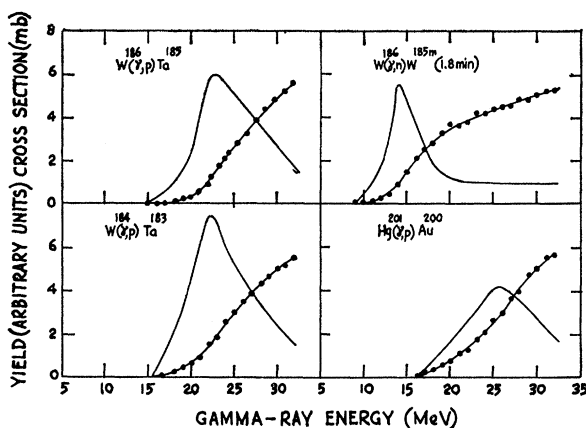


FIG. 7. Excitation functions and derived cross sections for the photodisintegration of tungsten and mercury.

irradiations. The decay schemes proposed in the Nuclear Data Sheets and elsewhere<sup>24</sup> were used to obtain the absolute yields. End-window Geiger counters were used to count the  $\beta^-$  particles of 74-day  $W^{185}$ , the absolute yields being determined by the methods of Baker and Katz.<sup>25</sup>

The measured yield curves are shown in Fig. 7. A complete excitation function was not obtained for the production of 74-day  $W^{184}$ , the yield of which was measured at a few high-energy points only. Excitation functions for the other reactions were measured at 1-MeV intervals. The yield curves were analyzed<sup>26</sup> by matrix inversion to obtain the cross section curves of Fig. 7. Some important parameters of these cross sections are summarized in Table I. The integrated cross section for  $W^{186}(\gamma, n)W^{185}$  (74 day) has been obtained on the assumption that this cross section has the same shape as the  $W^{186}(\gamma, n)W^{185}$  (1.8 min) cross section. Because of the smoothing effect of integration, this assumption is believed not to introduce errors exceeding the  $\pm 20\%$  assigned to all integrated cross sections in Table I.

<sup>24</sup> R. K. Gergis, R. A. Ricci, and R. van Lieshout, Nuclear Phys. **14**, 589 (1959).

<sup>25</sup> R. G. Baker and L. Katz, Nucleonics **11**, (2), 14 (1953).

<sup>26</sup> We are indebted to Mr. D. W. Lang for writing the program for this analysis, which was performed on SILLIAC.